Original Paper

phys. stat. sol. (b) **244**, No. 5, 1735–1742 (2007) / **DOI** 10.1002/pssb.200675113

Characterization of growth defects in thin GaN layers with X-ray microbeam

R. I. Barabash[*, 1], **G. E. Ice**[1], **C. Roder**[2], **J. Budai**[1], **W. Liu**[3], **S. Figge**[2], **S. Einfeldt**[**, 2], **D. Hommel**[2], and **R. F. Davis**[4]

[1] Materials Science & Technology Div., Oak Ridge National Laboratory, Oak Ridge, TN, 37831, USA
[2] Institute of Solid State Physics, University of Bremen, P.O. Box 330 440, 28334 Bremen, Germany
[3] Advanced Photon Source, Argonne IL, USA
[4] Materials Science and Engineering Department, North Carolina State University, Raleigh, USA

Received 4 September 2006, accepted 5 January 2007
Published online 4 April 2007

PACS 42.62.–b, 61.10.–i, 61.72.Dd, 61.72.Ff, 68.55.Ln

The spatially resolved distribution of strain, misfit and threading dislocations, and crystallographic orientation in uncoalesced GaN layers grown on Si(111) by maskless cantilever epitaxy or by pendeo epitaxy on SiC was studied by white beam Laue X-ray microdiffraction, scanning electron and orientation imaging microscopy. Tilt boundaries formed at the column/wing interface depending on the growth conditions. A depth dependent deviatoric strain gradient is found in the GaN. The density of misfit dislocations as well as their arrangement within different dislocation arrays was quantified. Two different kinds of tilt (parallel and perpendicular to the stripe direction) manifested themselves by mutually orthogonal displacements of the (0006) GaN Laue spot relative to the Si(444) Laue spot. The origin of the tilts is discussed with respect to the miscut of the Si(111) surface and misfit dislocations formed at the interface. Regular oscillations of the conventional wing tilt were observed. Irregular crystallographic tilts fluctuations were found in the direction parallel to stripes. The amplitude of fluctuations is an order of magnitude smaller for layers with a lower defects density.

© 2007 WILEY-VCH Verlag GmbH & Co. KGaA, Weinheim

1 Introduction

A high density of threading dislocations (typically 10^8–10^{10} cm^{-2}) is usually found in GaN films grown on different substrates [1–4]. Various lateral epitaxial overgrowth (LEO) techniques have recently been developed which greatly reduce the density of threading dislocations. One of them is cantilever epitaxy (CE) with GaN wings overhanging over the trenches produced in Si substrates by photolithography methods [5–9]. Very often the laterally grown wings are found to be crystallographically tilted. This wing tilt is crucial as it can result in dislocations or cracks at the coalescence point of the wings. In this paper, our previous work on CE GaN grown on Si(111) substrates [9, 10] is continued with the objective to the depth-resolved measurements. Our previous analysis indicates that a strain gradient forms with depth in the GaN layer. In this study we address this issue explicitly. Comparison of the results obtained by different methods such as polychromatic X-ray microdiffraction (PXM), high resolution X-ray diffraction (HRXRD), scanning electron microscopy (SEM), and FE simulations allows us to obtain detailed information about the depth-dependent local microstructural distribution of strain, lattice rotations and misfit dislocations density in GaN layers grown by CE on Si(111) substrates.

* Corresponding author: e-mail: barabashr@ornl.gov, Phone: 865 241 7230, Fax: 865 574 7659
** Present address: Ferdinand-Braun-Institut, Gustav-Kirchhoff-Str. 4, 12489 Berlin, Germany

WILEY InterScience® DISCOVER SOMETHING GREAT

© 2007 WILEY-VCH Verlag GmbH & Co. KGaA, Weinheim

2 Experimental details

The two samples under investigation (A and B) are identical to those presented in Refs. [9] and [10]. The Si(111) substrate consists of about 4.5 µm wide ridges separated by about 5.0 µm wide trenches in the Si[11$\bar{2}$] direction. The substrate was overgrown with a 100 nm thick AlN nucleation layer followed by a thick GaN layer using metal-organic vapor phase epitaxy. The growth was stopped before the coalescence of the GaN wings, resulting in separate GaN stripes in the GaN[1$\bar{1}$00] direction. The direction perpendicular to the GaN stripe in the plane of the film coincides with the GaN[11$\bar{2}$0] direction. The two samples differ in their wing tilt as they were grown under different growth conditions which resulted in a different ratio of the vertical and lateral growth rate during the initial GaN overgrowth. Further details of the growth process can be found in Refs. [7] and [8].

Polychromatic X-ray microdiffraction (PXM) was used for spatially resolved structural investigations. PXM was performed with a focused ~0.5 µm diameter polychromatic synchrotron beam which intersects the sample surface at 45° incidence. The Laue diffraction patterns from both the GaN layer and the Si substrate were recorded with a charge-coupled device (CCD) area detector placed at an angle of 90° relative to the incident beam [11–13] (Fig. 1). To obtain depth resolved information about the strain distribution in the GaN layers we performed measurements with the so called DAXM technique [13] (Fig. 1).

With DAXM, a three-dimensional map of the local crystallographic orientation and elastic strain tensor distributions in a sample can be determined. The three dimensional orientation distributions can be used to directly determine the dislocation tensor. Further details on the experimental setup, the data collection and quantitative analysis of diffraction profiles in PXM and DAXM can be found elsewhere [11–13].

The samples were also characterized by scanning electron microscopy (SEM) and by orientation imaging microscopy (OIM) using the field emission microscope of a FEI NOVA 200 focused ion beam system. The substrate miscut was measured by aligning the substrate Si(333) planes with the ϕ axis of a conventional Huber four-circle diffractometer and then observing the movement of a HeNe laser beam reflected from the sample surface. FE simulations of thermally induced strains were conducted using the software Flexpde 4.

3 Results and discussion

Figure 2 shows SEM images and OIM analysis (red insets) of both samples. The almost constant color for sample B confirms that surface orientation essentially does not change across the stripe in the sample B. In sample A the color changes in the region surrounding wing/column interface are observed, indicat-

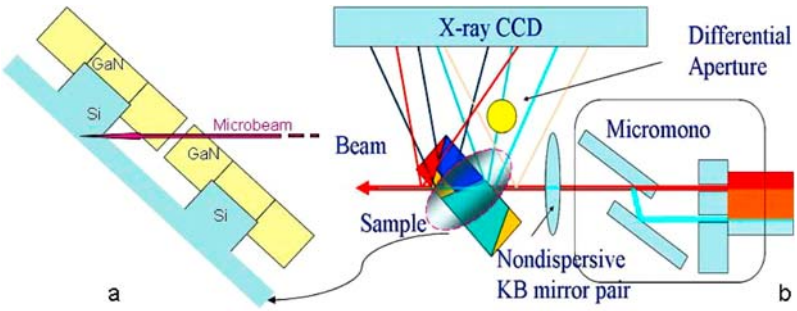

Fig. 1 (online colour at: www.pss-b.com) Geometry of mutual orientation of the microbeam and GaN layer (a) and a scheme of the differential "wire" technique (DAXM) used in PXM for depth resolved measurements.

© 2007 WILEY-VCH Verlag GmbH & Co. KGaA, Weinheim

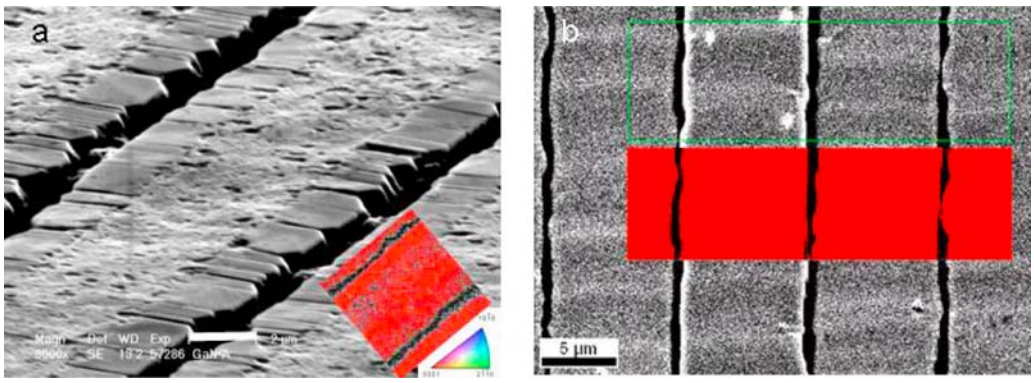

Fig. 2 (online colour at: www.pss-b.com) SEM and OIM (color inserts) images of the two CE grown GaN layers: (a) sample A and (b) sample B.

ing changes of orientation in this region. Many surface features oriented perpendicular to the stripes are also observed in Fig. 2a for sample A. The measurements of the substrate miscut revealed that the Si(111) planes for both samples have a surface miscut angle of 2.59°. The direction of the substrate miscut lies essentially in the direction parallel to the stripes, and we believe it is responsible for this component of the GaN film tilt. In this direction, the GaN[0001] axis was observed to be oriented between the Si[111] axis and the surface normal for both samples. In sample A, the GaN[0001] axis was tilted 1.6° away from the Si[111] axis, while the tilt was 0.68° for sample B. The buffer layer *c*-axis was found to be aligned parallel to the GaN axis at least for sample A. The measured *c* lattice parameter of 5.115 Å was closer to the lattice parameter for GaN ($c = 5.185$ Å) than to AlN ($c = 4.98$ Å), and suggests significant Ga diffusion into the buffer layer.

A typical PXM image for sample A is shown in Fig. 3a. Due to the large penetration depth of the X-rays, the Si reflections are superimposed on those from the GaN for every PXM image. Our previous PXM analysis of mutual orientation of the Si and GaN Laue spots obtained at different locations across the stripe indicated an upward tilt of the (0001) lattice planes of the GaN wing regions relative to the column by an angle of ~0.6° for sample A and 0.036° for sample B [10]. These findings by spatially-resolved PXM were in good agreement with the results of macroscopic HRXRD measurements. The corresponding values extracted from the reciprocal space maps (RSM) are 0.58° and 0.036° for sample A and B respectively. However in HRXRD the spot size of the X-ray beam is large (~0.5 mm), i.e. the

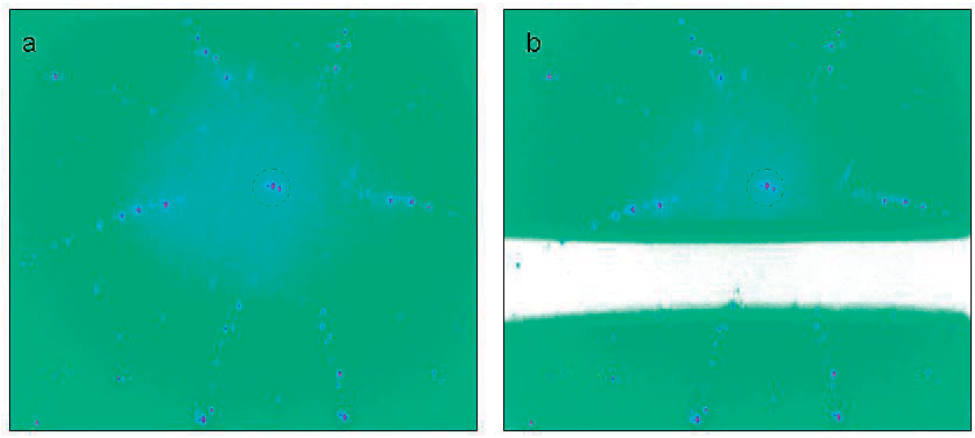

Fig. 3 (online colour at: www.pss-b.com) Total Laue pattern (a) and a pattern shadowed with a wire using DAXM technique (b) from the wing region of the sample A.

 © 2007 WILEY-VCH Verlag GmbH & Co. KGaA, Weinheim

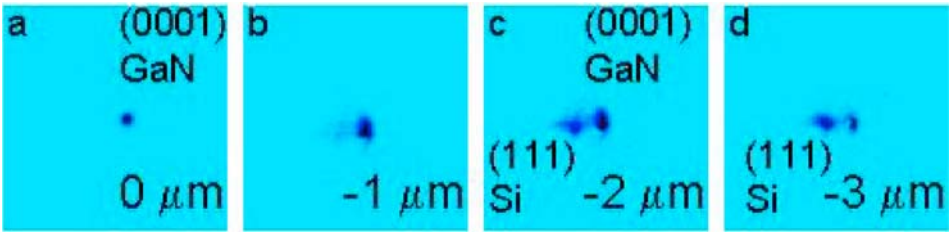

Fig. 4 (online colour at: www.pss-b.com) Several depth-resolved (reconstructed) images corresponding to the central part of the Laue pattern (dashed circle in Fig. 3a) demonstrate changes of GaN(0001) and Si(111) plane orientation with depth. Each step is 1 μm. Figure 4a is closest to sample surface.

RSM gives averaged information over ~50 stripes. In contrast, PXM provides spatially resolved information about the local structure at different positions across each stripe. The coincidence between the values of the wing tilt obtained by PXM and HRXRD shows that the local wing tilt is relatively homogeneous over the samples (although some fluctuations were observed mainly for sample A).

In this study, PXM images were obtained in a geometry with the stripe direction perpendicular to the beam (Fig. 1a). The total Laue pattern contains zone lines formed by GaN and Si Laue reflections (Fig. 3a). With the DAXM technique, the wire shadows part of the diffracted intensity (Fig. 3b). Images collected with different wire positions can be used to reconstruct the Laue images corresponding to different depth of the sample (Fig. 4). The dashed circle marks the area of interest containing the GaN(0006) and Si(444) reflections. Reconstructed depth-resolved Laue images (Fig. 4) of the central part of the Laue pattern demonstrate that there is a gradient of the orientation with depth. The direction of the GaN(0001) plane normal close to the surface (Fig. 4a) is distinct from the Si(111) substrate in agreement with the miscut measurements. However there is a narrow transition layer with a gradual change of orientations between the GaN and Si substrate (observed as a streak between the GaN and Si Laue spots in Fig. 4c). PXM provides information about the local shear strain since a lattice distortion causes streaking of the Laue reflections. The lattice curvature is caused by the elastic as well as plastic distortion of the lattice due to threading dislocations (TD) starting at the film/substrate interface and usually running through the GaN layer along the growth direction and misfit dislocations (MD) formed in the GaN layer. Similar to HRXRD, the impact of certain dislocations on a particular PXM reflection depends on the relative orientation of the Burgers vector and the diffraction vector. For instance, the GaN(0006) reflection will be broadened by screw-type TDs but not edge-type TDs. However, edge-type MDs running in the growth plane may significantly broaden the GaN(0006) reflection. The full width at half maximum along this streak, ξ, $\mathrm{FWHM}_{\xi} \propto n^{\mathrm{MD}} L f_{\xi}(\boldsymbol{\tau} \cdot \boldsymbol{G}_{hkl})$ depends on the reciprocal lattice vector for the (hkl) reflection $\boldsymbol{G}_{hkl}$, the size of the probed region L, the unit vector running, τ in the direction of the edge MDs, and on the so called PXM contrast factor f_{ξ}. The contrast factor f_{ξ} depends on the mutual orientation between $\boldsymbol{G}_{hkl}$ and the type of MDs slip systems operating in the probed region [12]. For a single slip system of edge MDs $f_{\xi}(\boldsymbol{\tau} \cdot \boldsymbol{G}_{hkl}) = \sqrt{1 - \cos^2(\boldsymbol{\tau} \cdot \boldsymbol{G}_{hkl})}$. The contrast factor reaches its maximum value of unity for edge dislocations running perpendicular to the reciprocal lattice vector [12].

The arrangement of dislocations as groups in walls may not only broaden a certain reflection but may result in its splitting into several peaks. From the splitting of GaN Laue reflections in the depth integrated images, the misorientation caused by the tilt boundary was determined. The spacing between dislocations in the boundary can be derived using the Burgers relation for a small angle tilt boundary $\vartheta = b/h$. Here ϑ is the tilt angle through the boundary, b is the Burgers vector of the dislocations forming the boundary, and h is the spacing between the dislocations in the boundary. Similar to the Ref. [10] we assume that the boundary is mainly formed by pure edge MDs (type 1) with a Burgers vector $\boldsymbol{b} = 1/3\langle 11\bar{2}0\rangle$ perpendicular to the stripes and dislocation lines running parallel to the stripes. This is a reasonable approximation as it is known that typically edge dislocations group in boundaries while screw dislocations remain randomly distributed. The dislocations usually pile up along the [0001] direction. Using the experimentally

© 2007 WILEY-VCH Verlag GmbH & Co. KGaA, Weinheim

observed tilt angle of the boundary we obtain an average dislocation distance $h \sim 50c$ for the sample A. Here c is the lattice constant of GaN along the [0001] direction. The total density of the MDs in the column region of the sample A results in $n^{MD} \approx 3.8 \times 10^9$ cm^{-2}. This value for a dislocation density is similar to those observed in the column region by other authors in GaN-based light emitting diodes [1, 2].

PXM results for sample A also indicate the formation of tilt boundaries perpendicular to the stripes. The data is consistent with MDs (type 2) having Burgers vectors $\boldsymbol{b} = 1/3\langle 1\bar{2}10\rangle$ and $\boldsymbol{b} = 1/3\langle \bar{2}110\rangle$. They are believed to pile up along the [0001] direction. The experimentally observed tilt angle of the boundary results in an average distance of the dislocations in the column of sample A of $h \sim 55c$. These dislocations are similar to the findings of Liliental-Weber et al. [18] and Sakai et al. [19].

The local structural quality of the GaN layers was analyzed by PXM. The small PXM microbeam (~0.5 μm) makes it possible to characterize the local structural information from different regions of the stripe. Figure 5 presents the results of mapping both kinds of tilt across seven stripes for samples A and B. Wing tilt in the direction perpendicular to the stripes (Fig. 5a, c) demonstrates regular oscillations. The amplitude of the wing tilt oscillations slightly changes from stripe to stripe in both samples, and for sample B it is an order of magnitude smaller than in sample A. In contrast in the direction parallel to stripes irregular fluctuations both in the amplitude and sign of the tilt are observed for sample A (Fig. 5b). At the smaller length scale (an order of magnitude smaller than for sample A) similar fluctuations are observed in the sample B (Fig. 5d).

FE simulations were performed to determine the contribution of the thermally induced elastic stress to the wing tilt. The thickness of the Si(111) substrate was set to 25 μm, which was tested to be sufficiently large to obtain realistic stresses in the GaN. The bottom surface of the Si was fixed against displacements along the x- and y-axes. The AlN layer between the GaN and the Si was omitted for simplicity. The strain was assumed to be induced during cooling of the structure from the growth temperature to room temperature ($\Delta T = 1063$ K) by the mismatch in the thermal expansion coefficients between GaN and Si. The latter data were taken from Refs. [14] and [15], respectively. For the stiffness constants of GaN and Si the values published in Refs. [16] and [17] were used. FE simulations predict an upward displacement

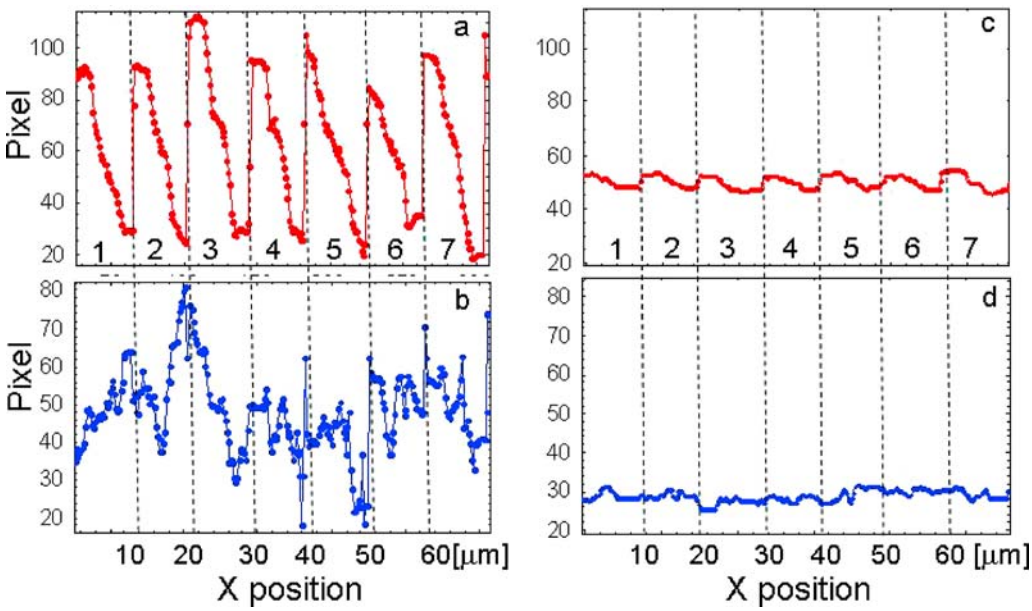

Fig. 5 (online colour at: www.pss-b.com) Regular wing tilt oscillations perpendicular to columns (a, c) and irregular crystallographic tilt fluctuations in the direction parallel to stripes (b, d) for sample A (a, b) and sample B (c, d).

 © 2007 WILEY-VCH Verlag GmbH & Co. KGaA, Weinheim

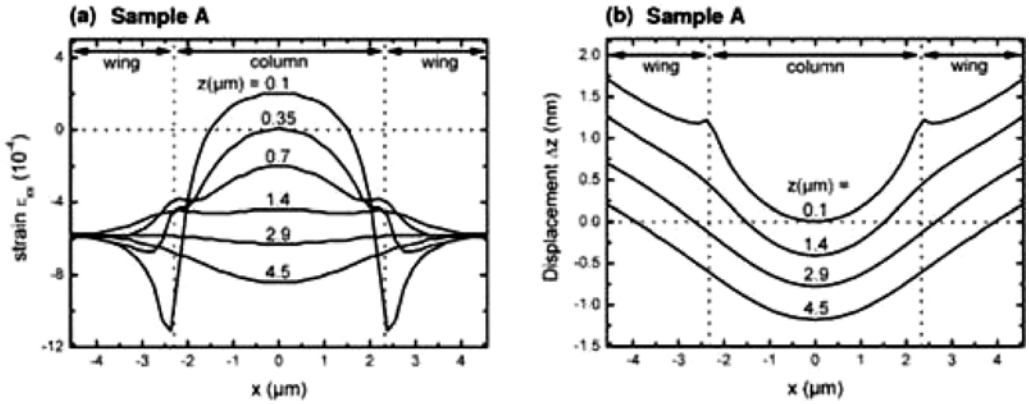

Fig. 6 Results of FE simulations for a thermal load of $\Delta T = 1063$ K of sample. The normal strain, ε_{XX}, along the x-direction (a) and the displacement along the z-direction (b) at different distances from the GaN/Si interface on top of the ridges ($z = 0$) are shown as line-scans in the x-direction across the stripe.

along the z-direction in the wing region relative to the column depending on the distances z from the top surface of the Si ridges (Fig. 6b). The normal in-plane strain (Fig. 6a) perpendicular to the stripe direction, ε_{XX}, changes sign at the wing/column interface at small distances from the Si substrate. The difference in strain between the wings and column regions decreases with the thickness of the GaN layer. Similar distribution of strain and displacements are found for sample B. It should be noted that for both samples, A and B, the absolute wing tilt measured at room temperature is much larger than the thermally induced wing tilt suggested by the FE simulations. This also agrees with the PXM data presented in this study.

We further consider the intrinsic stress relaxation during the CE growth of the GaN layer. It is well-known that heteroepitaxial layers can be crystallographically tilted with respect to their lattice-mismatched vicinal substrates (miscut 2.59° in our case). Several models have been proposed to explain the driving force for such a tilt [20–25]. Whereas Nagai considered the mismatch at surface steps of a vicinal substrate which favors a tilted growth to minimize the strain energy at the layer/substrate interface [22], Dodson and Tsao [23] have proposed misfit dislocations with inclined Burgers vectors as the source of the crystallographic tilt. The disclination dipoles model was proposed to explain the formation of lattice rotations between growing cells [25].

The Nagai model was recently applied in the interpretation of the crystallographic tilting of GaN layers epitaxially grown on vicinal surfaces of SiC [24]. In the following, the Dodson–Tsao [23] relaxation approach together with the Nagai mechanism [22] will be applied to the CE growth of GaN on miscut Si substrates to explain the origin of the crystallographic tilt parallel and perpendicular to the stripes.

The Nagai tilt can be calculated as $\tan\beta = -(\delta^z \tan\theta_y)$. Here, the AlN nucleation layer is neglected for simplicity and only the net effect of the step height differences, $\delta^z = -0.17$, corresponding to the lattice mismatch between Si and GaN in the z-direction is included. Since the impact of the in-plane lattice mismatch is much smaller than the out-of-plane mismatch the former is also omitted for simplicity. The measured value of the miscut angle $\theta_y = 2.59°$ results in the Nagai tilt of $\Delta\theta^{\text{Nagai}} \approx 0.5°$. For sample B, the experimental tilt parallel to the stripes is close to this value, $\Delta\theta^{\text{B}} \approx \Delta\theta^{\text{Nagai}}$. For sample A, the experimentally observed tilt parallel to the stripes is significantly larger than the Nagai tilt, $\Delta\theta^{\text{A}} \approx 1.6° \approx 3\Delta\theta^{\text{Nagai}}$. This means that a second tilt mechanism with biased nucleation and motion of misfit dislocations is important for sample A. We conclude that sample A possesses crystallographic tilt parallel to the stripes due to both the Nagai tilt and the biased misfit dislocation formation and hence has a higher dislocation density than sample B. Faceted growth is observed in SEM image (Fig. 7a). The growing (0001) facets are tilted relative to the surface normal. The model of dislocation arrangement and wing tilt is presented in Fig. 7b.

© 2007 WILEY-VCH Verlag GmbH & Co. KGaA, Weinheim

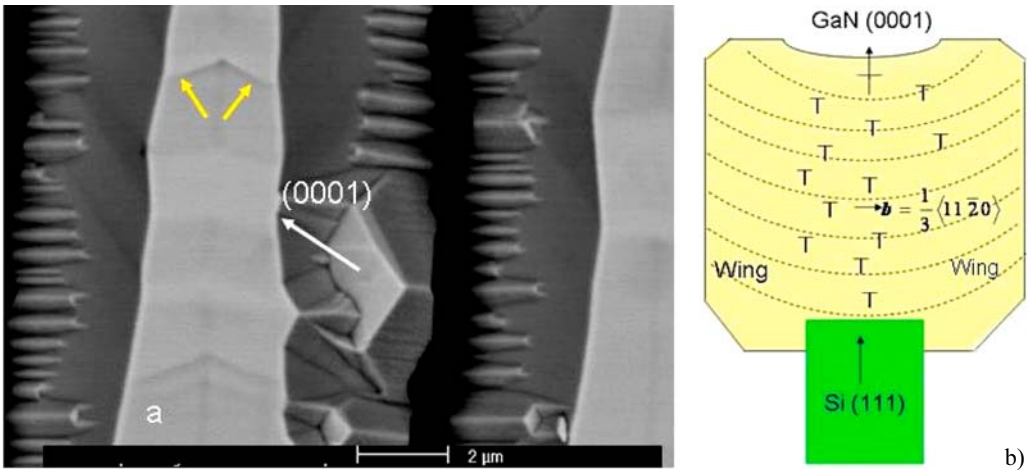

Fig. 7 (online colour at: www.pss-b.com) Faceted growth in the CE grown samples: SEM image (a) and a model of the lattice planes orientation (b). Yellow arrows in (a) show the formation of the tilt in the direction parallel to stripes.

4 Conclusions

PXM and DAXM analysis have been used in a 3D spatially-resolved investigation of the local lattice orientation and defect microstructure in GaN films grown on Si(111) by maskless CE. PXM reveals two different kinds of crystallographic tilts which are present to varying degrees in both samples. First, there is an upward tilt of the GaN wings in the direction perpendicular to the stripes. Second, a tilt in the direction parallel to the stripes is observed. Both kinds of tilt were found to be significantly larger in the sample which lacked sidewall deposition. Regular oscillations of the wing tilt were observed across different stripes. In contrast the amplitude and sign of the tilt parallel to stripe direction fluctuates irregularly from strip to stripe. This difference is due to the periodicity of the trenches in the substrate. Finite element simulations showed that extrinsic thermal stress relaxations provide only a minor contribution to the wing tilts. The X-ray Laue spots were analyzed in terms of strain-induced dislocations. The tilt parallel to the stripe direction was attributed to a substrate miscut and was analyzed in terms of a combination of elastic strain at surface steps and misfit dislocations formed at the interface.

Acknowledgements The research was supported in part by the U.S. Department of Energy, Division of Materials Science and Engineering through a contract with the Oak Ridge National Laboratory. Oak Ridge National Laboratory (ORNL) is operated by UT-Battelle, LLC, for the U.S. Department of Energy under contract DE-AC05-00OR22725. Data collection with PXM has been carried out on beamline ID-34-E at the Advanced Photon Source, Argonne IL. The APS is supported by the U.S. DOE, Basic Energy Sciences, Office of Science under contract No. W-31-109-ENG-38. This work was further supported by the Deutsche Forschungsgemeinschaft under Contracts No. HE 2827/5-1 and HO 1388/25-2. It is a pleasure to acknowledge T. M. Katona, J. S. Speck, and S. P. DenBaars from the University of California at Santa Barbara for growing the samples studied in this paper.

References

[1] S. Nakamura, phys. stat. sol. (a) **176**, 15 (1999).
[2] T. Hino, S. Tomiya, T. Miyajima, S. Hashimoto, and M. Ikeda, Appl. Phys. Lett. **76**, 3421 (2000).
[3] T. Miyajima, M. Taleya, S. Goto, S. Tomiya, S. Takeda, H. Kurihara, K. Watanabe, M. Kato, N. Hara, Y. Tsusaka, and J. Matsui, phys. stat. sol. (b) **240**, 285 (2003).
[4] N. Gmeinwieser, K. Engl, P. Gottfriedsen, U. T. Swarz, J. Zweck, W. Wegschneider, S. Miller, H.-J. Lugauer, A. Leber, A. Weimar, A. Lell, and V. Harle, J. Appl. Phys. **96**, 3666 (2004).

 © 2007 WILEY-VCH Verlag GmbH & Co. KGaA, Weinheim

[5] C. I. H. Ashby, C. C. Willan, J. Han, N. A. Missert, P. P. Provencio, D. M. Follstaedt, G. M. Peake, and L. Griego, Appl. Phys. Lett. **77**, 3233 (2000).
[6] A. Strittmatter, S. Rodt, L. Reissmann, D. Bimberg, H. Schröder, E. Obermeier, T. Riemann, J. Christen, and A. Krost, Appl. Phys. Lett. **78**, 727 (2001).
[7] T. M. Katona, M. D. Craven, P. T. Fini, J. S. Speck, and S. P. DenBaars, Appl. Phys. Lett. **79**, 2907 (2001).
[8] T. M. Katona, J. S. Speck, and S. P. DenBaars, Appl. Phys. Lett. **81**, 3558 (2002).
[9] C. Roder, H. Heinke, D. Hommel, T. M. Katona, J. S. Speck, and S. P. DenBaars, J. Phys. D, Appl. Phys. **36**, A188 (2003).
[10] R. I. Barabash, C. Roder, G. E. Ice, S. Einfeldt, J. D. Budai, O. M. Barabash, S. Figge, and D. Hommel, J. Appl. Phys. **100**, 053103 (2006).
[11] R. Barabash, G. Ice, B. Larson, G. Pharr, K. Chung, and W. Yang, Appl. Phys. Lett. **79**, 749 (2001).
[12] R. Barabash and G. Ice, Microdiffraction Analysis of Hierarchical Dislocation Organization, in: Encyclopedia of Materials: Science and Technology Updates (Elsevier, Oxford, 2005), pp. 1–18.
[13] B. C. Larson, W. Yang, G. E. Ice, J. D. Budai, and J. Z. Tischler, Nature **415**, 887 (2002).
[14] C. Roder, S. Einfeldt, S. Figge, and D. Hommel, Phys. Rev. B **72**, 085218 (2005).
[15] R. R. Reeber and K. Wang, Mater. Chem. Phys. **46**, 259 (1996).
[16] A. F. Wright, J. Appl. Phys. **82**, 2833 (1997).
[17] H. J. McSkimin, J. Appl. Phys. **24**, 988 (1953).
[18] Z. Liliental-Weber and D. Cherns, J. Appl. Phys. **89**, 7833 (2001).
[19] A. Sakai, H. Sunakawa, and A. Usui, Appl. Phys. Lett. **73**, 481 (1998).
[20] S. Einfeldt, D. Hommel, and R. F. Davis, in: Vacuum Science and Technology: Nitrides as Seen by the Technology, edited by T. Paskovaand and B. Monemar (Research Signpost, Trivandrum, 2002), pp. 147–166.
[21] J. D. Budai, W. Yang, N. Tamura, J. S. Chung, J. Z. Tischler, B. C. Larson, G. E. Ice, C. Park, and D. P. Norton, Nature Mater. **2**, 487 (2003).
[22] H. Nagai, J. Appl. Phys. **45**, 3789 (1974).
[23] B. W. Dodson and J. Y. Tsao, Appl. Phys. Lett. **51**, 1325 (1987); **52**, 852 (1988).
[24] X. R. Huang, J. Bai, M. Dudley, B. Wagner, R. F. Davis, and Y. Zhu, Phys. Rev. Lett. **95**, 086101 (2005).
[25] A. E. Romanov, P. Fini, and J. S. Speck, J. Appl. Phys. **93**, 106 (2003).

© 2007 WILEY-VCH Verlag GmbH & Co. KGaA, Weinheim